Chemokinetic Scattering, Trapping, and Avoidance of Active Brownian Particles

Justus A. Kromer,[1] Noelia de la Cruz,[2] and Benjamin M. Friedrich[3,4,5,*]
[1]Department of Neurosurgery, Stanford University, Palo Alto, California 94304, USA
[2]Department of Physics, McGill University, Montreal, Quebec H3A 2T8, Canada
[3]cfaed, TU Dresden, 01069 Dresden, Germany
[4]Institute of Theoretical Physics, TU Dresden, 01069 Dresden, Germany
[5]Cluster of Excellence Physics of Life, TU Dresden, 01307 Dresden, Germany

(Received 18 April 2019; revised manuscript received 3 December 2019; accepted 21 February 2020; published 17 March 2020)

We present a theory of chemokinetic search agents that regulate directional fluctuations according to distance from a target. A dynamic scattering effect reduces the probability to penetrate regions with high fluctuations and thus reduces search success for agents that respond instantaneously to positional cues. In contrast, agents with internal states that initially suppress chemokinesis can exploit scattering to increase their probability to find the target. Using matched asymptotics between the case of diffusive and ballistic search, we obtain analytic results beyond Fox colored noise approximation.

DOI: 10.1103/PhysRevLett.124.118101

Many motile cells can navigate in concentration gradients of signaling molecules in a process termed chemotaxis [1], which guides foraging bacteria to food patches, immune cells to inflammation sites, or sperm cells to the egg. Both chemotaxis close to targets and random search in the absence of guidance cues have been intensively studied; see Refs. [2–4] for reviews. Yet, navigation at intermediate distances from a target, where chemical cues provide no directional information but only indicate the proximity of a target, have received less attention. The regulation of speed and persistence of motion as a function of absolute concentration of signaling molecules is known as *chemokinesis* [1]. Chemokinesis offers a promising navigation strategy for artificial microrobots with minimal information processing capabilities [5,6].

In biological cells, chemotaxis and chemokinesis usually occur together, making it difficult to disentangle their effects. At the microscopic scale of cells, molecular shot noise compromises cellular concentration measurements, rendering cellular steering responses stochastic at low chemoattractant concentrations [7]. We can decompose stochastic steering responses as a superposition of directed steering and position-dependent directional fluctuations.

As an illustration, we consider a typical chemotaxis scenario, sperm cells of marine invertebrates [8]. There, the egg releases a chemoattractant, which establishes a radial concentration field $c(\mathbf{x})$ by diffusion [9]; see Fig. 1(a). Sperm cells can estimate the direction of the local concentration gradient ∇c, yet the signal-to-noise ratio (SNR) $\sim|\nabla c|^2/c$ of gradient sensing decreases as a function of radial distance $R=|\mathbf{x}|$; see Fig. 1(b). A previous, generic model of chemotaxis in the presence of sensing noise predicts stochastic steering responses with position-dependent directional fluctuations characterized by an effective rotational diffusion coefficient $D_{\rm rot}(\mathbf{x})$ [9]; see Fig. 1(c). Remarkably, $D_{\rm rot}\sim c/(c+c_b)^2$ becomes maximal at a characteristic distance from the target, marking a "noise zone" that incoming cells have to cross [9,10]. At this distance, absolute chemoattractant concentrations are above the threshold $c_b\sim 10$ pM for sensory adaptation, yet SNR $\ll 1$ (for details, see Ref. [9] or Supplemental Material (SM) [11]).

Motivated by this example, we pose the question of whether position-dependent directional fluctuations are beneficial or disadvantageous to find a target. This question is general: Spatial modulations of speed or directional fluctuations occur also in spatially inhomogeneous activity fields that influence the active motion of artificial microswimmers [17], or from the presence of obstacles [18,19]. Recent studies suggest an intriguing effect of position-dependent motility parameters on search success [17,20], termed "pseudochemotaxis" [21] in Refs. [22,23].

We emphasize that regulation of speed $v=v(\mathbf{x})$ as a function of position $\mathbf{x}$ (termed *orthokinesis* [1], considered previously in Refs. [22,23]) and regulation of the effective rotational diffusion coefficient $D_{\rm rot}=D_{\rm rot}(\mathbf{x})$ (*klinokinesis* [1], considered here) are equivalent: We can map orthokinesis on klinokinesis and vice versa, by a position-dependent time reparametrization of trajectories proportional to $v(\mathbf{x})^{-1}$. Such reparametrization changes conditional mean first passage times, but not the probability to find a target.

In this Letter, we develop a theory of chemokinetic search agents that regulate the level of directional fluctuations as a function of distance from a target. Our model generalizes active Brownian particles (ABPs), frequently used as a minimal model for cell motility, e.g., of biological or artificial microswimmers [24–26]. We characterize a dynamic scattering effect that reduces the probability to

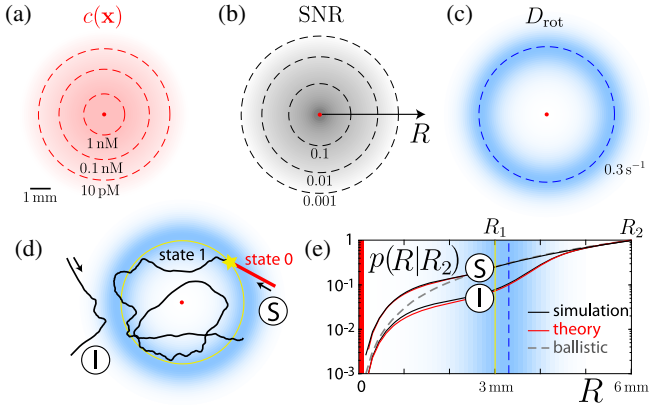

FIG. 1. Chemokinesis with position-dependent directional fluctuations as consequence of chemotaxis at low concentrations. (a) Radial concentration field $c(\mathbf{x})$ established by diffusion from a source (using parameters for sperm chemotaxis [9]): source (red dot), isoconcentration lines (dashed). (b) Computed signal-to-noise ratio (SNR) of chemotaxis decreases as function of radial distance R from the source. (c) The corresponding effective rotational diffusion coefficient $D_{\rm rot}$ displays a maximum at a characteristic distance (dashed), where $c(\mathbf{x})$ is still large, but SNR is low. (d) Simulated trajectory [labeled (I)] of a chemokinetic ABP subject to $D_{\rm rot}(\mathbf{x})$ from (c), corresponding to *instantaneous chemokinesis*. A second ABP [labeled (S)] with *two-state chemokinesis* initially moves ballistically (state 0), but switches to chemokinesis (state 1) as in (I) once it reaches a threshold distance (yellow) for the first time. Shown are two-dimensional reconstructions of three-dimensional trajectories obtained from numerical integration of Eqs. (1) and (2). (e) Penetration probability $p(R|R_2)$ that an ABP starting at distance R_2 reaches distance R before returning to R_2. For instantaneous chemokinesis (I), this probability is lower than for ballistic motion (dashed). For two-state chemokinesis (S), $p(R|R_2)$ is higher. Simulation results (black) compare favorably to our analytic theory (red). For parameters, see SM [11].

penetrate regions with high fluctuations. Using matched asymptotics between the limit cases of ballistic and diffusive motion, we develop an analytical theory of this scattering effect. Scattering always reduces the probability to find a target compared to a pure ballistic search for ABPs that respond instantaneously to positional cues. Yet, scattering substantially increases search success for ABPs with internal states that are able to suppress chemokinesis until they came close to the target for the first time, allowing these agents to realize multiple attempts to hit the target. The statistical physics of agents with instantaneous response and those with internal states is fundamentally different: while the former display a homogeneous mean residence time, this property is violated in the presence of internal states.

Adaptive active Brownian particles.—We consider an ABP moving along a trajectory $\mathbf{R}(t)$ in three-dimensional space with speed v and rotational diffusion coefficient $D_{\rm rot}$. Rotational diffusion causes its tangent $\mathbf{t} = \dot{\mathbf{R}}/v$ to decorrelate on a timescale $\tau_p = l_p/v$ set by the persistence length $l_p = v/(2D_{\rm rot})$, where dots denote time derivatives. Hence, $\langle \mathbf{t}(t_0) \cdot \mathbf{t}(t_0 + t) \rangle = \exp(-|t|/\tau_p)$ [27]. As a minimal model of chemokinesis with instantaneous regulation of motility, we consider ABPs that adjust speed and rotational diffusion coefficient as a function of position $\mathbf{x}$, $v = v(\mathbf{x})$ and $D_{\rm rot} = D_{\rm rot}(\mathbf{x})$. The steady-state density distribution for an ensemble of ABPs is independent of $D_{\rm rot}$ and inversely proportional to v (i.e., ABPs spend proportionally more time in locations, where they move slower), with isotropically distributed tangent directions.

Let a single spherical target of radius R_0 be located at $\mathbf{R} = 0$, and $v = v(|\mathbf{x}|)$, $D_{\rm rot} = D_{\rm rot}(|\mathbf{x}|)$. Because of spherical symmetry, the time-dependent distance $R(t) = |\mathbf{R}(t)|$ of a single ABP from the origin and the time-dependent angle $\psi(t)$ enclosed by its tangent $\mathbf{t}$ and the radial direction $\mathbf{e}_R = -\mathbf{R}/R$ decouple from other coordinates, see SM [11],

$$\dot{R} = -v \cos\psi, \tag{1}$$

$$\dot{\psi} = \frac{v}{R} \sin\psi + \sqrt{2D_{\rm rot}}\xi(t) + D_{\rm rot} \cot\psi. \tag{2}$$

Here, $\xi(t)$ is Gaussian white noise with $\langle \xi(t) \rangle = 0$ and $\langle \xi(t)\xi(t') \rangle = \delta(t - t')$.

Example: Directional fluctuations of chemotaxis.—We consider a chemokinetic ABP with constant speed v and position-dependent $D_{\rm rot}(\mathbf{x})$ as depicted in Fig. 1(c). We assume $R(t = 0) = R_2$ and random initial directions with direction angle ψ distributed according to $p(\psi) = \sin(2\psi)$ for $0 \le \psi \le \pi/2$, corresponding to the steady-state influx of ABPs at R_2 for random initial conditions outside R_2; see SM [11].

In Fig. 1(d), the trajectory labeled (I) is scattered back as soon as it encounters an elevated $D_{\rm rot}$. Indeed, the penetration probability $p(R|R_2)$ for such ABPs starting at distance R_2 to reach R before returning to R_2 is substantially lower than for ballistic motion with $D_{\rm rot} = 0$; see Fig. 1(e). For this case of *instantaneous chemokinesis*, directional fluctuations reduce the probability $p(R_0|R_2)$ to find the target.

In contrast, we may consider an ABP with two internal states [labeled (S) in Fig. 1(d)], which initially moves ballistically with $D_{\rm rot} = 0$ (state 0), and only upon crossing a boundary at R_1 switches on chemokinesis with $D_{\rm rot} = D_{\rm rot}(\mathbf{x})$ as in case (I) (state 1). For this *two-state chemokinesis*, directional fluctuations increase the probability to find a target; see Fig. 1(e). Next, we consider minimal models to explain this phenomenon.

Spatially inhomogeneous directional fluctuations cause dynamic scattering of ABP.—We first consider a minimal model with constant speed v and rotational diffusion coefficient $D_{\rm rot}(R)$ that is piecewise constant in zones concentric with the target, see Fig. 2(a):

$$D_{\rm rot}(R) = \begin{cases} D_1 & \text{for } R < R_1 (\text{zone } 1) \\ D_2 & \text{for } R \ge R_1 (\text{zone } 2). \end{cases} \tag{3}$$

We illustrate the effect of a spatially inhomogeneous rotational diffusion coefficient in two special cases, termed

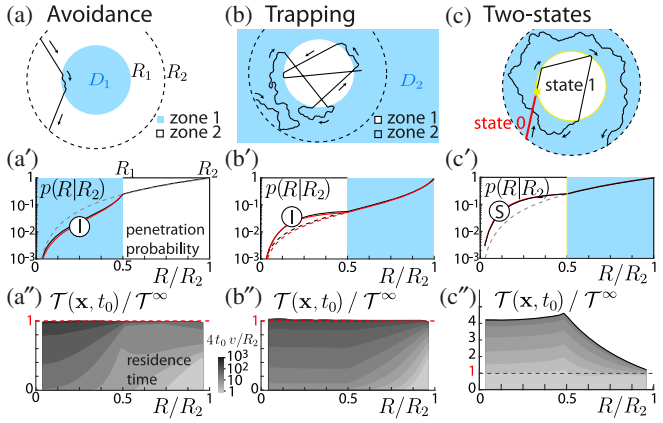

FIG. 2. Dynamic scattering of chemokinetic agents. (a) Trajectories entering zone 1 (blue) are scattered back to zone 2 due to a high rotational diffusion coefficient $D_1 > 0$ in zone 1. (a′) Penetration probability $p(R|R_2)$ that an ABP starting at distance R_2 reaches distance R before returning to R_2, analogous to Fig. 1(e): simulation (black), theory (red), ballistic motion with $D_1 = D_2 = 0$ (dashed). (a″) Residence time $\mathcal{T}(\mathbf{x}, t_0)$ at space position $\mathbf{x}$ before time t_0 as function of radial distance $R = |\mathbf{x}|$. By a mean-chord-length theorem, $\lim_{t_0\to\infty}\mathcal{T}(\mathbf{x}, t_0) = \mathcal{T}^\infty = (\pi R_2^2 v)^{-1}$. (b) Same as (a), but with $D_1 = 0$, $D_2 > 0$: trajectories can become trapped in zone 1 due to inward scattering of outgoing trajectories at R_1. (c) Same as (b), but for two-state chemokinesis: ABPs initially move ballistically with $D_{\rm rot} = 0$ (state 0), and switch to chemokinesis with $D_{\rm rot} = D_{\rm rot}(\mathbf{x})$ as in (b) after crossing a threshold distance (yellow) at R_1 (state 1). (c′) The penetration probability is higher compared to ballistic motion. (c″) The mean residence time is now spatially inhomogeneous. Parameters, $R_1 = R_2/2$: (a) $D_1 = 10v/R_2$, $D_2 = 0$; (b) $D_1 = 0$, $D_2 = 10v/R_2$; reference case (dashed) in (b′) $D_1 = D_2 = 10v/R_2$.

avoidance and *trapping* [1]; see Figs. 2(a) and 2(b). ABPs start at $R = R_2$ with random inward pointing initial direction angles ψ and terminate once they reach R_2 again.

If the ABP increases $D_{\rm rot}$ upon entering zone 1, most trajectories that enter zone 1 promptly return to zone 2, being scattered back due to the decrease in directional persistence; see Fig. 2(a).

Again, the penetration probability $p(R|R_2)$ for this case is lower than for ballistic motion, see Fig. 2(a′): most ABPs avoid zone 1. However, the ensemble-averaged residence time $\mathcal{T}(\mathbf{x})$ at each position $\mathbf{x}$ (with units time per volume) is spatially homogeneous, and equals the value $\mathcal{T}^\infty$ for ballistic motion. This is a direct corollary of the fact that the steady-state probability density for Eqs. (1) and (2) is independent of $D_{\rm rot}$. Elementary geometry gives $\mathcal{T}^\infty = 4/(vS)$ with $S = 4\pi R_2^2$ [28].

Thus, the mean residence time of *inhomogeneous* persistent random walks is the same as the mean residence time for ballistic motion. This extends a prominent result for *homogeneous* stochastic motion [29,30], also known as the mean-chord-length property, which found applications for wave scattering [31] and modeling of neutron transport [32]. The original proof can be adapted to inhomogeneous stochastic motion, asserted in Ref. [33]. Related results were discussed for position-dependent translational diffusion [6,21,34].

Intuitively, although most trajectories are reflected away from zone 1, a small fraction of trajectories will penetrate into zone 1 and dwell there an extended period of time before eventually leaving. Figure 2(a″) shows a time-bounded residence time $\mathcal{T}(\mathbf{x}, t_0)$ to find an ABP at position $\mathbf{x}$ at distance R before time t_0 [with $\lim_{t_0\to\infty}\mathcal{T}(\mathbf{x}, t_0) = \mathcal{T}(\mathbf{x})$].

If the ABP instead increases $D_{\rm rot}$ when leaving zone 1, trajectories that have just left zone 1 may be scattered back; see Fig. 2(b). ABPs are "trapped" in zone 1. Concomitantly, $p(R|R_2)$ is higher than for spatially homogeneous persistent random walks with $D_1 = D_2 > 0$; see Fig. 2(b′). Again, $\mathcal{T}(\mathbf{x}) = \mathcal{T}^\infty$; see Fig. 2(b″). Intuitively, although some trajectories become trapped, many trajectories are scattered back to R_2 before they ever enter zone 1.

The case in Fig. 2(a) corresponds to chemokinetic avoidance [1]; imagine, zone 1 represents unfavorable conditions that agents seek to avoid: then, most agents will leave the unfavorable zone 1 fast, while a small number will suffer an adverse effect and spend more time in zone 1.

Instantaneous chemokinesis (I) versus two-state chemokinesis (S).—To characterize the role of scattering for target search, we introduce the return probability $p_{\rm ret}$ to reenter zone 1 after entering zone 2 at $R = R_1$ (with random outward-pointing initial direction) and analogous zone-crossing probabilities $p_1 = p(R_0|R_1)$ and $p_2 = p(R_1|R_2)$; see Fig. 3(a). The probability $p(R_0|R_2)$ for ABPs with instantaneous chemokinesis starting at R_2 to hit the target of radius R_0 can be expressed in terms of these zone-crossing probabilities as a geometric series:

$$p(R_0|R_2) \approx \sum_{k=0}^{\infty} p_2[(1-p_1)p_{\rm ret}]^k p_1. \tag{4}$$

Here, the kth summand denotes the probability of successful trajectories that cross R_1 exactly $2k+1$ times. The only

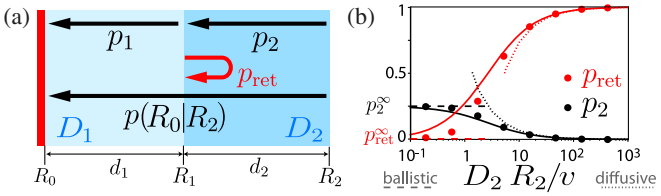

FIG. 3. Analytic theory by matched asymptotics. (a) The probabilities p_1 and p_2 to pass zone 1 and 2, respectively, and the return probability $p_{\rm ret}$ at the boundary between zone 1 and 2, jointly determine the probability $p(R_0|R_2)$ to reach a target of radius R_0 for ABPs starting at R_2; see Eq. (4). (b) Trade-off between p_2 (black) and $p_{\rm ret}$ (red) as function of D_2. Simulation (dots), limit of high $D_{\rm rot}$ (dotted), ballistic motion [Eq. (5)] (dashed), matched asymptotics [Eq. (6)] (solid).

assumption made in deriving Eq. (4) is a stereotypical distribution of direction angles at zone boundaries. Equation (4) corroborates that inward scattering at R_1 implies effective trapping of trajectories in zone 1, allowing for multiple attempts to hit the target.

Generally, p_i is a monotonically decreasing function of D_i, see Fig. 3(b), with maximal value p_i^∞ obtained for ballistic motion:

$$p_i^\infty = \lim_{D_i \to 0} p_i = \left(\frac{R_{i-1}}{R_i}\right)^2, \qquad i = 1, 2. \tag{5}$$

Note that p_{ret} and p_2 both depend on D_2, and thus cannot be optimized independently, see Fig. 3(b): increasing D_2 increases scattering of outgoing trajectories (thus increasing p_{ret}), yet also increases scattering of incoming trajectories (thus decreasing p_2).

An ABP with two internal states can decouple scattering of incoming and outgoing trajectories. Analogous to Fig. 1(d), label (S), we assume that ABPs initially move ballistically with $D_{\mathrm{rot}} = 0$ (state 0). Upon first entering zone 1, ABPs permanently switch to state 1 and subsequently obey Eq. (3); see Fig. 2(c). Figure 2(c′) demonstrates a dramatic increase of $p(R|R_2)$. Concomitantly, $\mathcal{T}(\mathbf{x})$ is not homogeneous anymore; see Fig. 2(c″).

Analytical theory.—We derive approximate analytical expressions for the return probability p_{ret} using matched asymptotics (p_1 and p_2 are analogous). Results compare favorably to simulations; see Fig. 2.

An ABP entering zone 2 from zone 1 at time $t = 0$ initially continues moving in approximately radial direction, before its direction of motion decorrelates on a timescale $\tau_p = (2D_2)^{-1}$. For times $t \gg \tau_p$, the ABP exhibits isotropic random motion. We treat these two dynamic phases separately and introduce a crossover time t_0 with $\tau_p \ll t_0 \ll D_2(d_2/v_0)^2$.

For the first phase, we are interested in the *penetration depth* $\langle x(t)\rangle$, i.e., the conditional expectation value of radial position $R_1 + x$ of ABPs that have not yet been absorbed at R_1 at time t. Let $Q(t)$ be the corresponding survival probability. In the limit $l_2 \ll R_1$, we can approximate the absorbing spherical shell at R_1 by a plane H. Using symmetry of renewal processes under reflection at H, we compute $\lim_{t\to\infty}\langle x(t)\rangle Q(t) = \alpha l_2$ with $\alpha = 4/3$; see SM [11]. Intuitively, while fewer and fewer ABPs survive, their mean distance from H diverges as $\langle x(t)\rangle \approx \alpha l_2/Q(t) \sim \alpha l_2 (t/\tau_p)^{1/2}$.

We now address the second dynamic phase $t \geq t_0$ and calculate p_{ret}. Those ABPs that have not been absorbed at R_1 before t_0 will likely be found at a distance $x \gg l_2$ from R_1, and we may approximate these as diffusive particles. The probability that a diffusive particle reaches R_2 if released at radial position R between two absorbing spherical shells of radii R_1 and R_2 reads $p(R) = (R_2/R)(R - R_1)/(R_2 - R_1)$ [7]. Choosing $R = R_1 + \langle x(t_0)\rangle \approx R_1 + \alpha l_2/Q(t_0)$ yields an asymptotic result for $q = 1 - p_{\mathrm{ret}}$ as $q \approx Q(t_0)p[R(t_0)]$, valid for $\lambda_2 \ll (\tau_p/t_0)^{1/2}$. Here, we introduced the ratios $\lambda_i = l_i/d_i$ between the persistence length $l_i = v/(2D_i)$ inside zone i and zone width $d_i = R_i - R_{i-1}$, $i = 1, 2$.

We can extend this asymptotic expression to the entire range $0 < \lambda_2 < \infty$ by interpolating with the limit value $q^\infty = \lim_{\lambda_2\to\infty} 1 - p_{\mathrm{ret}} = 1$ for ballistic motion, using the simple ansatz of a saturation curve $q \approx \gamma\lambda_2 q^\infty/[q^\infty + \gamma\lambda_2]$, with initial slope γ. We find

$$p_{\mathrm{ret}} \approx (1 + \alpha\lambda_2 R_2/R_1)^{-1}, \qquad \alpha = 4/3. \tag{6}$$

Analogously, $p_i \approx \alpha\lambda_i p_i^\infty R_{i-1}/(R_i p_i^\infty + \alpha\lambda_i R_{i-1})$, $i = 1, 2$ [recall $\lambda_i = v/(2D_i d_i)$].

Continuum limit.—By induction, we can generalize the minimal model of Eq. (3) with $n = 2$ zones to the case of $n > 2$ zones concentric with the origin bounded by $R_{i-1} < R \leq R_i$, $i = 1, \ldots, n$. From Eqs. (4) and (6), we obtain a recursion relation for $p(R_0|R_i)$; see SM for details [11]. In the continuum limit $n \to \infty$, we obtain a differential equation for $p(R_0|R)$, describing the penetration probability for the case of instantaneous chemokinesis, where $D_{\mathrm{rot}} = D_{\mathrm{rot}}(R)$ may be an arbitrary function of R:

$$\frac{\partial}{\partial R} p(R_0|R) = -2\frac{p}{R} - D_{\mathrm{rot}}(R)\frac{3}{2}\frac{p^2}{v}. \tag{7}$$

By definition, $p(R_0|R_0) = 1$. We conclude that for instantaneous chemokinesis, the probability to find a target is always smaller compared to ballistic motion. For two-state chemokinesis with threshold distance at R_1, the penetration probability equals $p^\infty(R|R_2)$ for $R_1 \leq R < R_2$, and differs from $p(R|R_2)$ by a factor $p^\infty(R_1|R_2)/p(R_1|R_2) > 1$ for $R < R_1$; see Fig. 2(c′).

Discussion.—Using a minimal model of a chemokinetic agent that regulates its rotational diffusion coefficient D_{rot} as a function of distance from a target, we explain how search agents can harness spatially inhomogeneous directional fluctuations to find targets more efficiently if they possess internal states.

This chemokinesis strategy exploits a dynamic scattering effect that scatters agents away from regions where directional fluctuations are high. Agents that have just missed the target and move on an outgoing trajectory can thus become scattered inward again and realize an additional search attempt. Yet, agents with instantaneous chemokinesis face a trade-off between this beneficial inward scattering of outgoing trajectories and unwanted outward scattering of incoming trajectories. Agents can avoid this trade-off if they suppress chemokinesis when approaching the target for the first time. In our minimal model, this strategy is realized by agents with two internal states, which could be implemented by a bistable switch, see SM [11]; alternatively, sensorial delay, memory, or hysteresis could serve a similar purpose.

Scattering is a genuinely dynamic effect. Consequently, the probability to find a target in spatially inhomogeneous systems cannot be predicted from mass-action laws on the basis of ensemble-averaged mean residence times. This highlights a fundamental difference between the dynamical and the steady-state behavior of spatially inhomogeneous active systems [22,23].

The dynamic scattering effect described here explains the increased target encounter rates previously observed for a spatially heterogeneous search of particles switching between ballistic and diffusive runs [20,35], as well as a search in spatially inhomogeneous activity fields [17,23] (using the mapping between klinokinesis and orthokinesis, see Introduction).

Our work connects to a recent interest in composite search strategies [2,36–39]. While most authors considered agents that stochastically switch between different levels of directional fluctuations, switching is triggered by the proximity to a target in our case, representing a *resource-sensitive* composite search [39,40].

In addition to chemokinesis studied here, chemotaxis can become useful in the ultimate vicinity of the target, where the signal-to-noise ratio of gradient sensing exceeds one, thus setting an effective target size. Our theoretical work suggests that single-molecule sensitivity of chemotactic cells [41] may in fact be disadvantageous during the initial approach to a target surrounded by a static, radial concentration field. Single-molecule sensitivity would be advantageous only later, once cells have passed a noise zone, where the concentration of signaling molecules equals the cell's sensitivity threshold. As an experimental test, chemotactic responses of cells with single-molecule sensitivity could be compared before and after exposure to high concentrations.

J. A. K. and B. M. F. are supported by the German National Science Foundation (DFG) through the Excellence Initiative by the German Federal and State Governments (Clusters of Excellence cfaed EXC-1056 and PoL EXC-2068), as well as DFG Grant No. FR3429/3-1 to B. M. F.; N. d. l. C. acknowledges a RISE-Globalink Research Internship for support. We thank Rainer Klages, Jens-Uwe Sommer, and Steffen Lange for a critical reading of the manuscript.

*benjamin.m.friedrich@tu-dresden.de

[1] G. Fraenkel and D. Gunn, *The Orientation of Animals* (Dover, New York, 1961).
[2] O. Bénichou, C. Loverdo, M. Moreau, and R. Voituriez, Intermittent search strategies, Rev. Mod. Phys. **83**, 81 (2011).
[3] G. M. Viswanathan, M. G. E. Da Luz, E. P. Raposo, and H. E. Stanley, *The Physics of Foraging* (Cambridge University Press, Cambridge, England, 2011).
[4] L. Alvarez, B. M. Friedrich, G. Gompper, and U. B. Kaupp, The computational sperm cell, Trends Cell Biol. **24**, 198 (2014).
[5] M. Mijalkov, A. McDaniel, J. Wehr, and G. Volpe, Engineering Sensorial Delay to Control Phototaxis and Emergent Collective Behaviors, Phys. Rev. X **6**, 011008 (2016).
[6] L. G. Nava, R. Großmann, and F. Peruani, Markovian robots: Minimal navigation strategies for active particles, Phys. Rev. E **97**, 042604 (2018).
[7] H. C. Berg and E. M. Purcell, Physics of chemoreception, Biophys. J. **20**, 193 (1977).
[8] J. F. Jikeli, L. Alvarez, B. M. Friedrich, L. G. Wilson, R. Pascal, R. Colin, M. Pichlo, A. Rennhack, C. Brenker, and U. B. Kaupp, Sperm navigation along helical paths in 3D chemoattractant landscapes, Nat. Commun. **6**, 7985 (2015).
[9] J. Kromer, S. Märcker, S. Lange, C. Baier, and B. M. Friedrich, Decision making improves sperm chemotaxis in the presence of noise, PLoS Comput. Biol. **14**, e1006109 (2018).
[10] A. M. Hein, D. R. Brumley, F. Carrara, R. Stocker, and S. A. Levin, Physical limits on bacterial navigation in dynamic environments, J. R. Soc. Interface **13**, 20150844 (2016).
[11] See Supplemental Material at http://link.aps.org/supplemental/10.1103/PhysRevLett.124.118101 for additional details on analytical calculations, which includes Refs. [12–16].
[12] B. M. Friedrich and F. Jülicher, Steering Chiral Swimmers Along Noisy Helical Paths, Phys. Rev. Lett. **103**, 068102 (2009).
[13] A. Sharma, R. Wittmann, and J. M. Brader, Escape rate of active particles in the effective equilibrium approach, Phys. Rev. E **95**, 012115 (2017).
[14] R. Fox, Functional-calculus approach to stochastic differential equations, Phys. Rev. A **33**, 467 (1986).
[15] N. D. Kashikar, L. Alvarez, R. Seifert, I. Gregor, O. Jäckle, M. Beyermann, E. Krause, and U. B. Kaupp, Temporal sampling, resetting, and adaptation orchestrate gradient sensing in sperm, J. Cell Biol. **198**, 1075 (2012).
[16] M. Pichlo, S. Bungert-Pluemke, I. Weyand, R. Seifert, W. Boenigk, T. Strünker, N. D. Kashikar, N. Goodwin, A. Müller, H. G. Körschen *et al.*, High density and ligand affinity confer ultrasensitive signal detection by a guanylyl cyclase chemoreceptor, J. Cell Biol. **206**, 541 (2014).
[17] H. Merlitz, C. Wu, and J.-U. Sommer, Directional transport of colloids inside a bath of self-propelling walkers, Soft Matter **13**, 3726 (2017).
[18] O. Chepizhko and F. Peruani, Diffusion, Subdiffusion, and Trapping of Active Particles in Heterogeneous Media, Phys. Rev. Lett. **111**, 160604 (2013).
[19] J. Wang, D. Zhang, B. Xia, and W. Yu, Spatial heterogeneity can facilitate the target search of self-propelled particles, Soft Matter **13**, 758 (2017).
[20] K. Schwarz, Y. Schröder, B. Qu, M. Hoth, and H. Rieger, Optimality of Spatially Inhomogeneous Search Strategies, Phys. Rev. Lett. **117**, 068101 (2016).
[21] M. J. Schnitzer, Theory of continuum random walks and application to chemotaxis, Phys. Rev. E **48**, 2553 (1993).
[22] P. K. Ghosh, V. R. Misko, F. Marchesoni, and F. Nori, Self-Propelled Janus Particles in a Ratchet: Numerical Simulations, Phys. Rev. Lett. **110**, 268301 (2013).
[23] H. D. Vuijk, A. Sharma, D. Mondal, J.-U. Sommer, and H. Merlitz, Pseudochemotaxis in inhomogeneous active Brownian systems, Phys. Rev. E **97**, 042612 (2018).

[24] P. Romanczuk, M. Bär, W. Ebeling, B. Lindner, and L. Schimansky-Geier, Active Brownian particles, Eur. Phys. J. Spec. Top. **202**, 1 (2012).
[25] C. Bechinger, R. Di Leonardo, H. Löwen, C. Reichhardt, G. Volpe, and G. Volpe, Active particles in complex and crowded environments, Rev. Mod. Phys. **88**, 045006 (2016).
[26] B. M. Friedrich, Search along persistent random walks, Phys. Biol. **5**, 026007 (2008).
[27] H. E. Daniels, The statistical theory of stiff chains, Proc. R. Soc. Edinburgh A **63**, 290 (1952).
[28] K. M. Case and P. F. Zweifel, *Linear Transport Theory* (Addison-Wesley, Reading, MA, 1967).
[29] S. Blanco and R. Fournier, An invariance property of diffusive random walks, Europhys. Lett. **61**, 168 (2003).
[30] O. Bénichou, M. Coppey, M. Moreau, P. Suet, and R. Voituriez, Averaged residence times of stochastic motions in bounded domains, Europhys. Lett. **70**, 42 (2005).
[31] R. Pierrat, P. Ambichl, S. Gigan, A. Haber, R. Carminati, and S. Rotter, Invariance property of wave scattering through disordered media, Proc. Natl. Acad. Sci. U.S.A. **111**, 17765 (2014).
[32] A. Zoia, C. Larmier, and D. Mancusi, Cauchy formulas for linear transport in random media, Europhys. Lett. **127**, 20006 (2019).
[33] S. Blanco and R. Fournier, Short-Path Statistics and the Diffusion Approximation, Phys. Rev. Lett. **97**, 230604 (2006).
[34] A. W. C. Lau and T. C. Lubensky, State-dependent diffusion: Thermodynamic consistency and its path integral formulation, Phys. Rev. E **76**, 011123 (2007).
[35] K. Schwarz, Y. Schröder, and H. Rieger, Numerical analysis of homogeneous and inhomogeneous intermittent search strategies, Phys. Rev. E **94**, 042133 (2016).
[36] M. J. Plank and A. James, Optimal foraging: Levy pattern or process? J. R. Soc. Interface **5**, 1077 (2008).
[37] C. Loverdo, O. Bénichou, M. Moreau, and R. Voituriez, Robustness of optimal intermittent search strategies in one, two, and three dimensions, Phys. Rev. E **80**, 031146 (2009).
[38] F. Bartumeus, E. P. Raposo, G. M. Viswanathan, and M. G. da Luz, Stochastic optimal foraging: tuning intensive and extensive dynamics in random searches, PLoS One **9**, e106373 (2014).
[39] B. C. Nolting, T. M. Hinkelman, C. E. Brassil, and B. Tenhumberg, Composite random search strategies based on non-directional sensory cues, Ecol. Complexity **22**, 126 (2015).
[40] S. Benhamou, Efficiency of area-concentrated searching behaviour in a continuous patchy environment, J. Theor. Biol. **159**, 67 (1992).
[41] T. Strünker, L. Alvarez, and U. Kaupp, At the physical limit-chemosensation in sperm, Curr. Opin. Neurobiol. **34**, 110 (2015).